

pubs.acs.org/acscatalysis Letter

Decarbonylation of Carboxylic Acids over H-Mordenite

Ziqiao Zhou, Hongchao Liu, Zhiyang Chen, Wenliang Zhu,* and Zhongmin Liu*



Cite This: ACS Catal. 2021, 11, 4077-4083



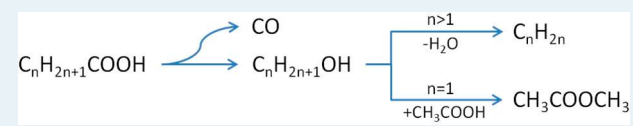
ACCESS

Metrics & More

Article Recommendations

Supporting Information

ABSTRACT: Decarbonylation of carboxylic acids is an effective reaction for alkene production but suffers from the requirement of homogeneous transitional-metal-based catalyst, ligand, and stoichiometric additive. Herein, we report the example of heterogeneous zeolite-catalyzed decarbonylation, in which acetic acid generates



methyl acetate with a selectivity close to 90%, while propionic and butanoic acid provide ethylene and propylene, respectively, both with a selectivity of about 70% over pyridine-modified H-MOR. Decarbonylation of acetic acid proceeds via the generation of methanol by the cleavage of carbonyl C=O from hydrogen-bonded acetic acid and the subsequent esterification to methyl acetate. Similarly, decarbonylation of propionic and butanoic acid correspondingly result in ethanol and propanol, which dehydrate rapidly to ethylene and propylene. This finding presents additional perspectives on decarbonylation of carboxylic acids and offers an approach for production of alkenes from biomass.

KEYWORDS: heterogeneous, decarbonylation, carboxylic acid, H-mordenite, acid-catalysis

ecarbonylation is an effective reaction to provide alkenes and has potential for renewable alkene production from carboxylic acids that could be abundantly found in bio-oil.^{2,3} Currently, alkenes are feedstock chemicals that are conventionally produced in a large scale by cracking in the petroleum industry and consumed tremendously in the manufacture of plastics and fine chemicals. Recently, Szostak et al. have revealed the importance of decarbonylation of carboxylic acids by demonstrating the capability for the production of various aromatics, 4-6 which are as important as alkenes. However, the utilization of decarbonylation is limited because it requires catalysts that contain transitional metals such as Ni, Pd, Ir, and Pd, among others, that are accompanied by an organic ligand and usually the addition of stoichiometric additive such as anhydride), and most of the reported decarbonylation reactions are homogeneous. 1,7-13 Up to now, the heterogeneous decarbonylation of carboxylic acids conducted without any transitional metal, ligand, or stoichiometric additive has not been reported.

Herein, we present the first example of zeolite-catalyzed heterogeneous decarbonylation of carboxylic acid. Acetic, propionic, and butanoic acid were employed and converted into methyl acetate, ethylene, and propylene, respectively, over pyridine-modified H-MOR without any participation of transitional metal, ligand, or stoichiometric additive.

Decarbonylation of acetic acid was tested over different zeolites, and the results are shown in Figure 1. These Hzeolites are used because of their different channel dimension and the size of the openings (Table.S1). For H-ZSM-5, H-ZSM-35, H-Beta, and H-Y, the primary product is acetone, indicating that ketonization of acetic acid majorly took place over these zeolites. H-MOR is also capable for ketonization, and the selectivity of acetone is about 9%; however, methyl

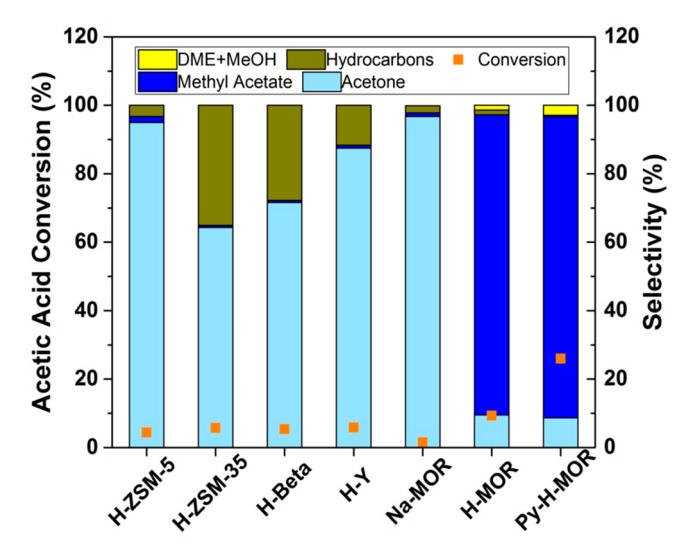


Figure 1. Results of decarbonylation of acetic acid over different zeolites at 240 min, 593 K, 1 bar, $P_{\text{acetic acid}} = 6 \text{ kPa}$, total GHSV = 3000 h⁻¹, and Ar was used as balancing gas.

acetate holds a large proportion in the product, and the selectivity reached 88%. It should be noted that neither dimethyl ether (DME) nor methanol was introduced in the reaction, but acetic acid was still converted into methyl acetate

Received: January 17, 2021 Revised: March 7, 2021 Published: March 17, 2021





directly. In contrast, DME and methanol could be found as products with a selectivity of \sim 3%. Additionally, there is no obvious conversion of acetic acid over Na-MOR; therefore, the significant difference in methyl acetate selectivity between H-MOR and Na-MOR indicates that the decarbonylation of acetic acid is an acid-catalyzed reaction.

Mordenite contains 8-membered ring channels (8M.R. 2.6 × 5.7 Å) and 12M.R. channels $(6.5 \times 7.0 \text{ Å})$ that are both parallel with the c axis, and 8M.R. and 12M.R. channels are connected by an 8M.R. passage $(3.4 \times 4.8 \text{ Å})$ along the b axis, which is also called the side pocket. 14 Acids in 12M.R. main channels and 8M.R. side pockets may behave differently in this reaction. Thus, pyridine treatment for H-MOR was used to differentiate their catalytic performances, and this procedure has been applied in the literature. 15-17 The difference between H-MOR and pyridine-treated H-MOR (denoted as py-H-MOR) can be observed by the IR spectra (Figure.S2). After pyridine treatment, the peak at 3600 cm-1 shifted and weakened to 3585 cm⁻¹, which were assigned to acids in the 12M.R. channel and the 8M.R. side pocket, respectively. 18-20 Results agree with recent literature that pyridine is able to hinder the acids in both the 12M.R. main channel and the 8M.R. side pocket, but pyridine that adsorped on acids located in the 8M.R. side pocket would desorb upon heating.² Therefore, only acids in the 8M.R. side pocket remain active for py-H-MOR. The result of the reaction over py-H-MOR is also presented in Figure 1. There is no significant difference in selectivity of methyl acetate between the two catalysts, but the conversion of acetic acid is even higher over py-H-MOR, indicating that the formation of methyl acetate is catalyzed by acids located within the 8M.R. side pocket of H-MOR and that pyridine acted as an acidity-modifier and did not catalyze the formation of methyl acetate.

The time-on-stream of the reaction over H-MOR and py-H-MOR is shown in Figure.S3. The conversion of acetic acid over H-MOR reaches a max of ~17% and then drops slowly, while that over py-H-MOR remains ~27%. The selectivity of methyl acetate over both catalysts is ~90%. Veefkind et al.²² have reported that the synthesis rates of ethylamine is ~1.5 times higher on H+ within the 8M.R. side pocket than those within 12M.R. channels, and Liu et al. 23,24 found a higher yield of methyl acetate over H-MOR in which the acids in the 12M.R. channel were removed. Similarly, it could be possible that the formation rate of methyl acetate is also faster in the 8M.R. side pocket than in the 12M.R. channel. As an acidity-modifier, pyridine restricts the reaction to take place only in the 8M.R. side pocket, and therefore, a higher yield of methyl acetate is obtained over py-H-MOR. Additionally, previous investigations have pointed out that acids in the 12M.R. main channels easily lead to the coke formation; ^{25,26} thus, the coke generated in the 12M.R. main channels would cause a drop in the conversion of acetic acid. TG analysis of spent H-MOR and py-H-MOR is shown in Figure.S4. The final weight percentages were 91.51% for py-H-MOR, 87.85% for H-MOR, and 92.4% for the fresh py-H-MOR. The results in TG analysis illustrated that there is more coke in spent H-MOR than in spent py-H-MOR. Thus, pyridine would deactivate acids in 12M.R. main channels of H-MOR, suppressing the coke production, and the conversion of acetic acid in 8M.R. side pocket is reserved.

The fracture of the acetyl group of acetic acid occurs in this reaction because the methoxy groups of methyl acetate are the C_1 components. It can be anticipated that the C-C breakage

produces an equal amount of C_1 product and CO, a reaction that is similar to the reversed direction of methanol carbonylation to acetic acid. As shown in Figure 2, carbon

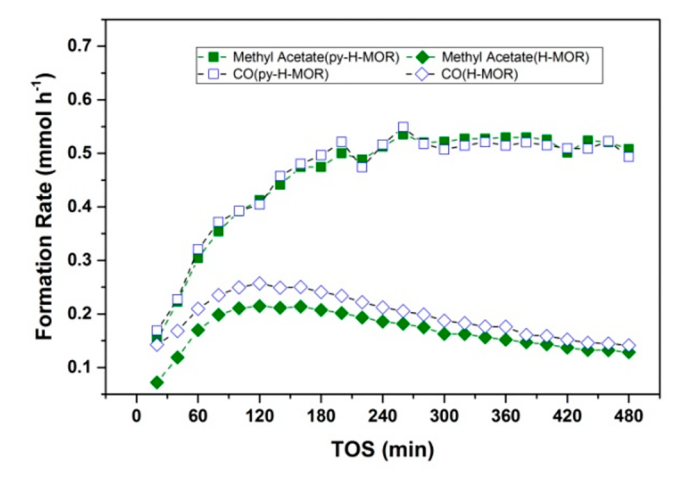


Figure 2. Formation rate of CO and methyl acetate over H-MOR and py-H-MOR. 593 K, 1 bar, $P_{\text{acetic acid}} = 6 \text{ kPa}$, total GHSV = 3000 h⁻¹, and Ar was used as balancing gas.

monoxide was detected in the effluent, and the flow rates of methyl acetate and CO were quite close. The ratios of CO flow rate to that of methyl acetate were about 1.14 and 1.01 over H-MOR and py-H-MOR, respectively (Figure.S5). The formation rate ratio indicates that the C–C bond in acetic acid breaks into equivalent CO and CH_3 –, and most CH_3 – in acetic acid eventually presented in the form of methyl acetate.

The effects of reaction conditions, including temperature, partial pressure of acetic acid and CO, and contact time, were studied. Decarbonylation of acetic acid is triggered at 553 K, and the selectivity of methyl acetate eventually reached and maintained at ~90% with increasing temperature (Figure 3a). Acetic acid becomes a reactant at the temperature that decarbonylation is activated. As shown in Figure.S6, ethyl

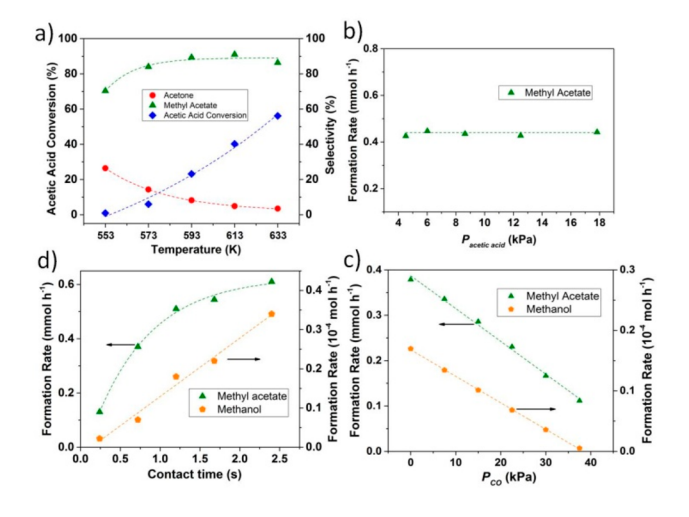


Figure 3. (a) Effect of temperature (1 bar, $P_{\text{acetic acid}} = 6 \text{ kPa}$, total GHSV = 3000 h⁻¹). (b) Effect of partial pressure of acetic acid (593 K, 1 bar, total GHSV = 3000 h⁻¹). (c) Effect of CO partial pressure (593 K, 1 bar, $P_{\text{acetic acid}} = 3.1 \text{ kPa}$, total GHSV = 4224 h⁻¹). d) Effect of contact time (593 K, 1 bar, $P_{\text{acetic acid}} = 6 \text{ kPa}$). Py-H-MOR was used as catalyst, and Ar was used as balancing gas.

acetate generated about the same selectivity of ethylene and acetic acid at 553 K, and about 7.2% selectivity of methyl acetate could be found when the temperature was 593 K, which succeeded in obtaining methyl acetate from ethyl acetate for the overall reaction. The formation rate of methyl acetate did not depend on the partial pressure of acetic acid, as presented in Figure 3b, which implies that strong adsorption of acetic acid took place. Formation rates of both methyl acetate and methanol (DME was counted as double methanol) were linearly ($R^2 = 0.99$) suppressed by CO (Figure 3c). The active sites for decarbonylation of acetic acid over py-H-MOR were the acids located in the 8M.R. side pocket of H-MOR, which was also selective for carbonylation of DME and methanol. 27,28 Previous studies have also demonstrated that increasing partial pressure of CO linearly increases the formation of methyl acetate²⁹ and also increases the selectivity ratio of acetic acid to methyl acetate. 17 Therefore, the negative kinetic relevance of CO partial pressure indicated that decarbonylation of acetic acid could be a reversible reaction and the CO was produced by the direct cleavage of carbonyl C=O from acetic acid.

The effect of contact time was studied to investigate the change of product distribution on the catalyst by adjusting the amount of catalysts. The formation rates of methyl acetate and methanol on different contact times are shown in Figure 3d (DME was counted as double methanol). The formation rate of methanol increases about linearly $(R^2 = 0.98)$ with the contact time, suggesting that methanol is involved neither with carbonylation nor esterification reaction and acted as a final product. However, most of the methanol participates in esterification, leading to the formation rate of methyl acetate at least ~25 times higher than that of methanol. The formation rate of methyl acetate can be fitted into the exponential function of the contact time $(y = 0.63 - 0.69 \exp(-1.39t), R^2 =$ 0.99), inferring the reversibility of the decarbonylation. The derivation of the reversibility is presented in Supporting Information.

To study the migration of CH_3 — of acetic acid during the reaction, methyl acetate derived from decarbonylation of fully deuterated acetic acid (CD_3COOD) was analyzed, and the GC-MS spectrum is compared with that of commercially obtained methyl acetate. Commercially obtained methyl acetate is used to represent the methyl acetate that generated from decarbonylation of acetic acid (CH_3COOH). As presented in Figure 4, the GC-MS spectrum of methyl acetate contains signals at m/e = 15, 43, 59, and 74, and they are the moiety of methoxy (CH_3), acetyl (CH_3CO), carboxyl (CH_3COO), and the molecule of methyl acetate itself,

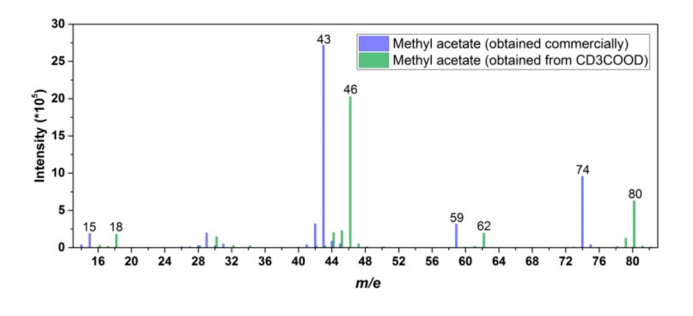


Figure 4. GC-MS spectrum of commercially obtained methyl acetate, and methyl acetate derived from decarbonylation of CD₃COOD. 603 K, 1 bar, $P_{\text{acetic acid}} = 6 \text{ kPa}$, total GHSV = 1500 h⁻¹, py-H-MOR was the catalyst, and Ar was used as balancing gas.

respectively. For methyl acetate that is derived from CD_3COOD , there are signals at m/e = 18, 46, 62, and 80, correspondingly, and they are the deuterated methoxy (CD_3) , acetyl (CD_3CO) , carboxyl (CD_3COO) , and fully deuterated methyl acetate (CD_3COOCD_3) . These results illustrate that one of participated acetic acids breaks itself into CO and methanol, and the latter undergoes esterification with another acetic acid to form methyl acetate.

The decarbonylation of acetic acid was also studied by in situ reflectance infrared Fourier transform (DRIFT) spectroscopy. As shown in Figure 5, after the adsorption of acetic acid

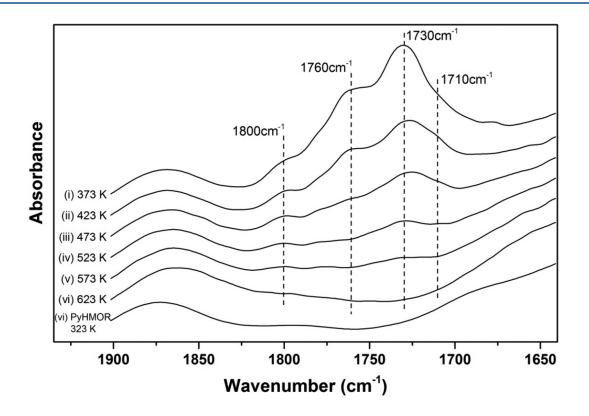


Figure 5. In situ DRIFT spectra of acetic acid on the Py-H-MOR sample from 373 to 623 K.

upon py-H-MOR, several new peaks appeared. The peak at 1800 cm⁻¹ is assigned to the weakly adsorped acetic acid, ³⁰ the band at $\sim 1730~\text{cm}^{-1}$ is assigned to C=O stretching of hydrogen-bonded acetic acid, 31,32 and the bands at 1760 and 1710 cm⁻¹ are assigned to surface acetyl species.^{28,33} All these peaks decline upon heating. However, it can be found that acetyl species weaken easier than the hydrogen-bonded acetic acid, which is evidenced by the disappearance of peaks at 1760 and 1710 cm⁻¹, while those at 1730 cm⁻¹ still partly remained at 573 K. Acetic acid primarily undergoes decarbonylation over py-H-MOR at such temperature, and it was pointed out that the surface acetyl species are found on zeolite and are responsible for ketone formation. 3,30,33-35 Therefore, the selective formation of methyl acetate instead of acetone over py-H-MOR should be attributed to the hydrogen-bonded acetic acid rather than acetyl species. Previous literature pointed out that the stable methoxy group can be formed within the 8M.R. side pocket of H-MOR, where the attack of CO to methoxy group is also favored by the unique orientation.²⁵ Consequently, it could be possible that the cleavage of CO from acetic acid is also favored in the same location; whether CO attacks the methoxy group or leaves from acetic acid depends on the CO partial pressure.

To further investigate the role of acids in the 8M.R. side pocket of H-MOR for this reaction, several NaH-MOR samples with different Na⁺ content were used to adjust the H⁺ concentration, and their IR spectra were recorded (Figure.S7). Because of the replacement of Na⁺, the intensity of the peaks at 3610 and 3589 cm⁻¹, which are assigned to –OH stretching in the 12M.R. main channel and the 8M.R. side pocket, respectively, ^{18–20} declines with increasing Na⁺ content. Na⁺ ion-exchange effects neither the MOR framework (Figure.S8) nor the surface area (Table.S2). The transformation of integrated peak area into the amount of

corresponding acids follows the reported research.³⁶ For pyridine-modified NaH-MOR samples, only acids in the 8M.R. side pocket are available for the reaction, and as shown in Figure 6, a quadratic correlation ($y = 34.3x^2 - 1.8x + 1.8x$

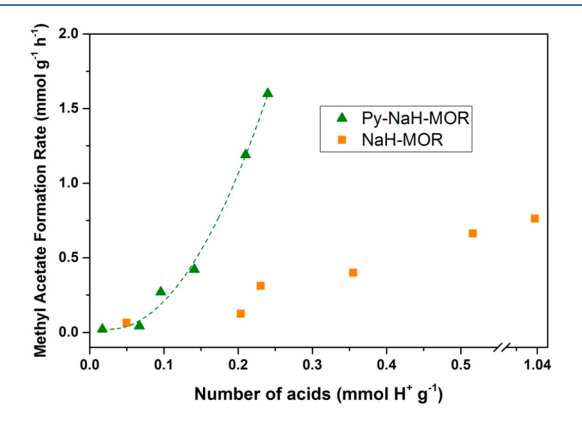


Figure 6. Methyl acetate formation rate per unit mass plotted against the number of acid sites per unit mass of pyridine-modified NaH-MOR (Py-NaH-MOR) and NaH-MOR. 593 K, 1 bar, $P_{\text{acetic acid}} = 6$ kPa, total GHSV = 3000 h⁻¹, and Ar was used as balancing gas.

0.04, $R^2 = 0.99$) could be found. Meanwhile, the formation rate of methyl acetate was also measured using NaH-MOR samples without pyridine treatment, where the acids in the 8M.R. side pocket and the 12M.R. main channel are both active. However, the formation rate of methyl acetate cannot establish a correlation with the number of acids in the 12M.R. main channel. Additionally it can be noticed that the formation of methyl acetate over Py-NaH-MOR increases more sharply than NaH-MOR; therefore, the conversion to coke from generated methyl acetate catalyzed by acids in the 12M.R. channel can be anticipated. These results further illustrate that the conversion of acetic acid to methyl acetate is catalyzed by acids in the 8M.R. side pocket of H-MOR, and pyridine acted as an acidity-modifier to avoid the consumption of methyl acetate.

Herein, by the above results, the equation of methyl acetate generation is composed of decarbonylation of acetic acid to methanol (eq 1) and the subsequent esterification of methanol with acetic acid (eq 2):

$$CH_3COOH = CH_3OH + CO$$
 (1)

$$CH_3OH + CH_3COOH = CH_3COOCH_3 + H_2O$$
 (2)

and the overall reaction (eq 3):

$$2CH3COOH = CH3COOCH3 + CO + H2O$$
 (3)

H-Mordenite catalyzed decarbonylation is also applicable to propionic acid. As shown in Figure 7, 3-pentone is found to be the major product over H-ZSM5, H-Beta, and H-Y, indicating that propionic acid undergoes ketonization and the subsequent conversion of 3-pentone to hydrocarbons. Contrarily, a considerable amount of ethylene was found with a selectivity of about 40% and 60% over H-MOR and H-ZSM35, respectively, and particularly 70% over py-H-MOR. The catalytic performance of py-H-MOR indicates that decarbonylation of propionic acid is catalyzed by acids within the 8M.R. side pocket of H-MOR, which can also be evidenced by the linear correlation (y = 2.7x + 0.07, $R^2 = 0.97$) between ethylene formation rate and the number of acids in the 8M.R.

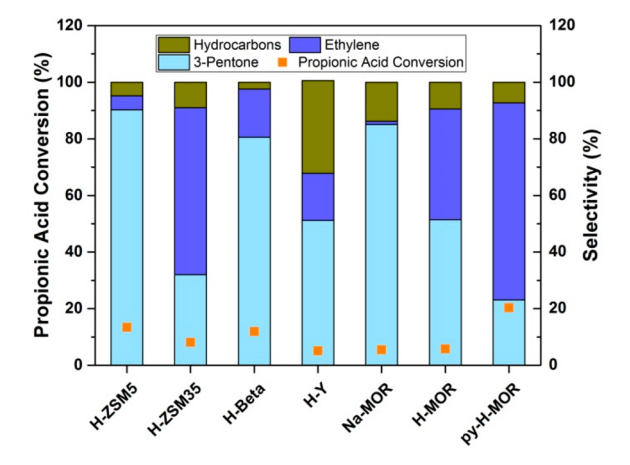


Figure 7. Decarbonylation of propionic acid over different H-zeolites at 180 min. 613 K, 1 bar, $P_{\text{propionic acid}} = 3 \text{ kPa}$, total GHSV = 3000 h⁻¹, and Ar was used as balancing gas.

side pocket (Figure.S9). Similar to the decarbonylation of acetic acid over py-H-MOR, CO was found in the effluent, and the flow rate of CO and ethylene was measured. The flow rates of CO and ethylene are very close, and the rate over py-H-MOR is much higher than over H-MOR (Figure.S10). The ratios of flow rates of CO to ethylene over H-MOR and py-H-MOR are ~1.3 and ~1.04, respectively (Figure.S11), which shows that propionic acid breaks into equal amounts of ethylene and CO. The CO/ethylene ratio over H-MOR is much higher than on py-H-MOR, which is caused by polymerization of ethylene into coke in the 12M.R. main channel of H-MOR.

As shown in Figure 7, ethylene can be also found over H-ZSM5, H-ZSM35, H-Beta, and H-Y, and their ratios of formation rate of CO to ethylene are 1.5, 1.1, 4, and 3 (Figure.S12), respectively. The ethylene formation over H-ZSM5, H-Beta, and H-Y is not associated with propionic acid decarbonylation because the ratio is much higher than 1. The significant ethylene selectivity over H-ZSM35 could be possibly due to the decarbonylation of propionic acid, because H-ZSM35 has FER cavities at the intersection of the 8 and 10M.R. channels, 14 and the similar size of the pore opening of the 8M.R. channel (3.5 × 4.8 Å) with the side pocket of H-MOR (3.4 × 4.8 Å); however, the exact reason for ethylene formation from propionic acid over H-ZSM35 deserves further study.

Decarbonylation of propionic acid was also studied in a similar way to acetic acid. Both propionic acid conversion and ethylene selectivity increased with temperature (Figure 8a). The effect of partial pressure of CO is shown in Figure 8b, and ethylene formation rate remains constant at different CO partial pressures. Neither the carbonylation of ethanol nor the Reppe reaction of ethylene takes place, and currently, the examples of these two reactions over H-MOR have not been reported. As shown in Figure 8c, increasing partial pressure of propionic acid promotes the formation of ethylene. The relation between formation rate and partial pressure agrees with the Langmuir isotherm $(y = 0.057x/(1 + 0.032x), R^2 =$ 0.98), indicating that there is an equilibrium between gaseous and adsorped propionic acid and the latter results in ethylene. Additionally, as presented in Figure 8d, the relation between ethylene formation and contact time is about linear $(R^2 =$ 0.98), and ethanol was not found in the effluent because of the

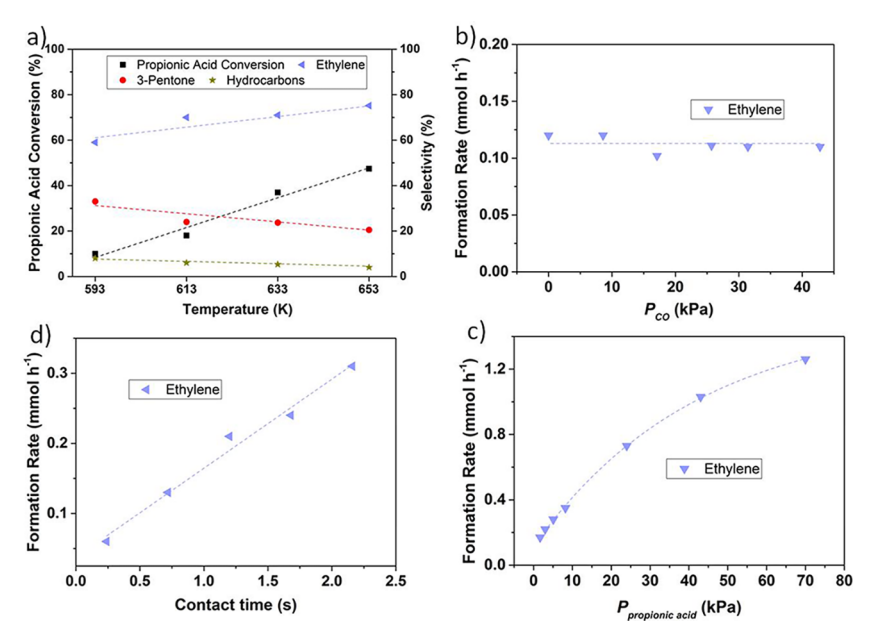


Figure 8. (a) Effect of temperature (1 bar, $P_{\text{propionic acid}} = 3 \text{ kPa}$, total GHSV = 3000 h⁻¹, TOS = 180 min). (b) Effect of partial pressure of CO (613 K, 1 bar, $P_{\text{propionic acid}} = 1.5 \text{ kPa}$, total GHSV = 4224 h⁻¹). (c) Effect of partial pressure of propionic acid (613 K, 1 bar, total GHSV = 3000 h⁻¹. (d) Effect of contact time (613 K, 1 bar, $P_{\text{propionic acid}} = 3 \text{ kPa}$). Py-H-MOR was used as catalyst and Ar as balancing gas.

dehydration of ethanol. The measured capacity of ethanol dehydration to ethylene under the same reaction condition is at least 100 mmol h^{-1} , because both ethanol conversion and ethylene selectivity are >99.9% (Figure.S13). However, the ethylene formation in propionic acid decarbonylation is about 1.2 mmol h^{-1} at most in this study, and therefore, ethanol is too short-lived to be observed. Similar to the decarbonylation of acetic acid to methyl acetate, the overall equation for the decarbonylation of propionic acid to ethylene is as follows (eq 4):

$$CH_3CH_2COOH = C_2H_4 + CO + H_2O$$
 (4)

Butanoic acid also undergoes decarbonylation reaction over py-H-MOR. As shown in Figure 9, propylene is found with a selectivity of about 70%, accompanied by ketonization to 4heptanone with a selectivity of about 22%. Similar to the decarbonylation of acetic and propionic acid, CO was detected

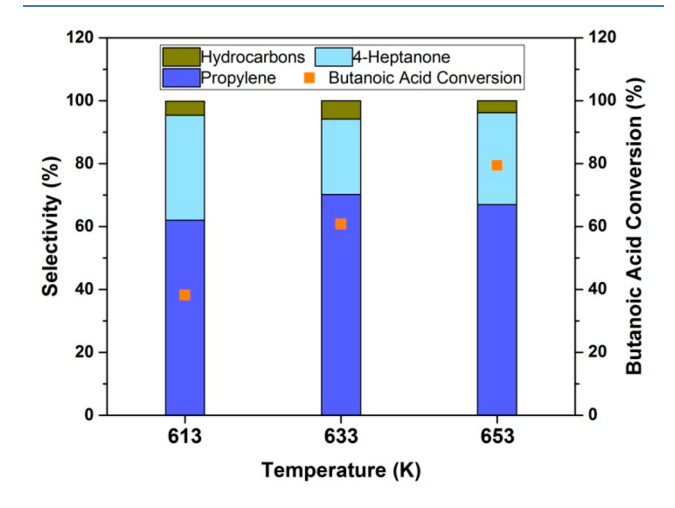


Figure 9. Decarbonylation of butanoic acid over py-H-MOR at TOS = 180 min. 1 bar, $P_{\text{butanoic acid}} = 6 \text{ kPa}$, total GHSV = 1875 h⁻¹, and Ar was used as balancing gas.

in the effluent, and the flow rate ratio of CO to propylene shows an average of about 1 (Figure.S14). Therefore, decarbonylation of butanoic acid is similar to the reaction of propionic acid. The overall equation (eq 5) could be written as

$$CH_3CH_2COOH = C_3H_6 + CO + H_2H$$
 (5)

On the basis of the results of decarbonylation of acetic, propionic, and butanoic acid, a mechanism is proposed. As shown in Scheme 1, decarbonylation of carboxylic acid

Scheme 1. Proposed Mechanism of Decarbonylation of Carboxylic Acid

$$C_{n}H_{2n+1}COOH \xrightarrow{CO} C_{n}H_{2n+1}OH \xrightarrow{n=1} CH_{3}COOCH_{3}$$

provides CO and one-carbon-less alkanol. Decarbonylation of acetic acid (n = 1) provides carbon monoxide and methanol, which consequently undergoes esterification to methyl acetate in the presence of acetic acid, while ethanol and propanol generated by decarbonylation of propionic and butanoic acid (n > 1), respectively, would dehydrate quickly to corresponding ethylene and propylene. Dehydration of methanol cannot provide alkene, and therefore, methyl acetate is produced. Contrarily, dehydration is very easy for ethanol and propanol, leading to the formation of alkenes instead of ester.

In conclusion, decarbonylation of carboxylic acids is achieved over H-MOR without any involvement of transitional metal, organic ligand, or stoichiometric additives. Decarbonylation of acetic acid provides methyl acetate at 593 K, and higher conversion of acetic acid can be obtained over pyridine-treated H-MOR. As an acidity modifier, pyridine deactivates acids in the 12M.R. main channel and consequently suppresses the coke formation. Studies including spectral and isotopic methods show that, catalyzed by acids within the 8M.R. side pocket of H-MOR, methanol is generated by direct and

reversible CO cleavage of a hydrogen-bonded acetic acid and quickly undergoes esterification with another adsorped acetic acid, which results in equal amounts of CO and methyl acetate. Similar to acetic acid, decarbonylation of propionic acid is also catalyzed by acids located in the 8M.R. side pocket of H-MOR, where the irreversible cleavage of CO from propionic acid provides ethanol followed by quick dehydration of ethanol to ethylene, and eventually, an equal amount of CO and ethylene is obtained. Decarbonylation of butanoic occurs in the same manner as propionic acid, and equal amounts of propylene and CO are found. Decarbonylation of C_2 – C_4 carboxylic acids over H-MOR provides an additional catalytic perspective for carboxylic acid removal and renewable alkene synthesis.

ASSOCIATED CONTENT

Solution Supporting Information

The Supporting Information is available free of charge at https://pubs.acs.org/doi/10.1021/acscatal.1c00235.

Experimental; Reversibility derivation for decarbonylation of acetic acid; channel dimension of zeolites used in this study; surface area and pore volume of NaH-MOR; XRD characterization of zeolites; IR spectra of H-MOR and py-H-MOR; time-on-stream of acetic acid decarbonylation; TG analysis of spent H-MOR and py-H-MOR; ratio of formation rate of CO to methyl acetate; reaction of ethyl acetate; IR spectra and Na+ content of NaH-MOR; XRD characterization of NaH-MOR; correlation between number of acids and ethylene formation rate; formation rate of CO and ethylene over H-MOR and py-H-MOR; ratio of formation rate of CO to ethylene over H-MOR and py-H-MOR; ratio of formation rate of CO to ethylene over H-ZSM5, H-ZSM35, H-Beta, and H-Y; capacity of ethanol dehydration over py-H-MOR; and formation rate of CO and propylene and the ratio of CO to propylene (PDF)

AUTHOR INFORMATION

Corresponding Authors

Wenliang Zhu — National Engineering Laboratory for Methanol to Olefins, Dalian National Laboratory for Clean Energy, iChEM, Dalian Institute of Chemical Physics, Chinese Academy of Sciences, Dalian 116023, P.R. China; Email: wlzhu@dicp.ac.cn

Zhongmin Liu — National Engineering Laboratory for Methanol to Olefins, Dalian National Laboratory for Clean Energy, iChEM, Dalian Institute of Chemical Physics, Chinese Academy of Sciences, Dalian 116023, P.R. China; University of Chinese Academy of Sciences, Beijing 100049, P.R. China; orcid.org/0000-0002-7999-2940; Email: liuzm@dicp.ac.cn

Authors

Ziqiao Zhou — National Engineering Laboratory for Methanol to Olefins, Dalian National Laboratory for Clean Energy, iChEM, Dalian Institute of Chemical Physics, Chinese Academy of Sciences, Dalian 116023, P.R. China; University of Chinese Academy of Sciences, Beijing 100049, P.R. China

Hongchao Liu – National Engineering Laboratory for Methanol to Olefins, Dalian National Laboratory for Clean Energy, iChEM, Dalian Institute of Chemical Physics, Chinese Academy of Sciences, Dalian 116023, P.R. China Zhiyang Chen — National Engineering Laboratory for Methanol to Olefins, Dalian National Laboratory for Clean Energy, iChEM, Dalian Institute of Chemical Physics, Chinese Academy of Sciences, Dalian 116023, P.R. China; University of Chinese Academy of Sciences, Beijing 100049, P.R. China

Complete contact information is available at: https://pubs.acs.org/10.1021/acscatal.1c00235

Author Contributions

All authors have given approval to the final version of the manuscript.

Funding

This study was financially supported by National Natural Science Foundation of China (Grant Nos. 21972141, 21978285, 21991090, and 21991094,), and the "Transformational Technologies for Clean Energy and Demonstration", Strategic Priority Research Program of the Chinese Academy of Sciences (Grant No. XDA21030100).

Notes

The authors declare no competing financial interest.

REFERENCES

- (1) Zhang, X.; Jordan, F.; Szostak, M. Transition-metal-catalyzed decarbonylation of carboxylic acids to olefins: exploiting acyl C–O activation for the production of high value products. *Org. Chem. Front.* **2018**, *5* (16), 2515–2521.
- (2) Han, Y.; Gholizadeh, M.; Tran, C.-C.; Kaliaguine, S.; Li, C.-Z.; Olarte, M.; Garcia-Perez, M. Hydrotreatment of pyrolysis bio-oil: A review. Fuel Process. Technol. 2019, 195, 106140.
- (3) Pham, T. N.; Sooknoi, T.; Crossley, S. P.; Resasco, D. E. Ketonization of Carboxylic Acids: Mechanisms, Catalysts, and Implications for Biomass Conversion. *ACS Catal.* **2013**, 3 (11), 2456–2473.
- (4) Liu, C.; Ji, C.-L.; Qin, Z.-X.; Hong, X.; Szostak, M. Synthesis of Biaryls via Decarbonylative Palladium-Catalyzed Suzuki-Miyaura Cross-Coupling of Carboxylic Acids. *iScience* **2019**, *19*, 749–759.
- (5) Liu, C.; Ji, C.-L.; Zhou, T.; Hong, X.; Szostak, M. Decarbonylative Phosphorylation of Carboxylic Acids via Redox-Neutral Palladium Catalysis. *Org. Lett.* **2019**, *21* (22), 9256–9261.
- (6) Liu, C.; Qin, Z.-X.; Ji, C.-L.; Hong, X.; Szostak, M. Highly-chemoselective step-down reduction of carboxylic acids to aromatic hydrocarbons via palladium catalysis. *Chemical Science* **2019**, *10* (22), 5736–5742.
- (7) Chatterjee, A.; Jensen, V. R. A Heterogeneous Catalyst for the Transformation of Fatty Acids to α -Olefins. *ACS Catal.* **2017**, 7 (4), 2543–2547.
- (8) John, A.; Dereli, B.; Ortuño, M. A.; Johnson, H. E.; Hillmyer, M. A.; Cramer, C. J.; Tolman, W. B. Selective Decarbonylation of Fatty Acid Esters to Linear α -Olefins. *Organometallics* **2017**, 36 (15), 2956–2964.
- (9) Lopez-Ruiz, J. A.; Pham, H. N.; Datye, A. K.; Davis, R. J. Reactivity and stability of supported Pd nanoparticles during the liquid-phase and gas-phase decarbonylation of heptanoic acid. *Appl. Catal., A* **2015**, *504*, 295–307.
- (10) John, A.; Hogan, L. T.; Hillmyer, M. A.; Tolman, W. B. Olefins from biomass feedstocks: catalytic ester decarbonylation and tandem Heck-type coupling. *Chem. Commun.* **2015**, *51* (13), 2731–2733.
- (11) John, A.; Miranda, M. O.; Ding, K.; Dereli, B.; Ortuño, M. A.; LaPointe, A. M.; Coates, G. W.; Cramer, C. J.; Tolman, W. B. Nickel Catalysts for the Dehydrative Decarbonylation of Carboxylic Acids to Alkenes. *Organometallics* **2016**, *35* (14), 2391–2400.
- (12) Ternel, J.; Lebarbé, T.; Monflier, E.; Hapiot, F. Catalytic Decarbonylation of Biosourced Substrates. *ChemSusChem* **2015**, 8 (9), 1585–1592.

- (13) Miranda, M. O.; Pietrangelo, A.; Hillmyer, M. A.; Tolman, W. B. Catalytic decarbonylation of biomass-derived carboxylic acids as efficient route to commodity monomers. *Green Chem.* **2012**, *14* (2), 490.
- (14) Moliner, M.; Martínez, C.; Corma, A. Multipore Zeolites: Synthesis and Catalytic Applications. *Angew. Chem., Int. Ed.* **2015**, *54* (12), 3560–3579.
- (15) Jiao, F.; Pan, X.; Gong, K.; Chen, Y.; Li, G.; Bao, X. Shape-Selective Zeolites Promote Ethylene Formation from Syngas via a Ketene Intermediate. *Angew. Chem., Int. Ed.* **2018**, *57* (17), 4692–4696
- (16) Liu, J.; Xue, H.; Huang, X.; Wu, P.-H.; Huang, S.-J.; Liu, S.-B.; Shen, W. Stability Enhancement of H-Mordenite in Dimethyl Ether Carbonylation to Methyl Acetate by Pre-adsorption of Pyridine. *Chinese Journal of Catalysis* **2010**, *31* (7), 729–738.
- (17) Ni, Y.; Shi, L.; Liu, H.; Zhang, W.; Liu, Y.; Zhu, W.; Liu, Z. A green route for methanol carbonylation. *Catal. Sci. Technol.* **2017**, 7 (20), 4818–4822.
- (18) Eder, F.; Stockenhuber, M.; Lercher, J. A. Brønsted Acid Site and Pore Controlled Siting of Alkane Sorption in Acidic Molecular Sieves. *J. Phys. Chem. B* **1997**, *101* (27), 5414–5419.
- (19) Maache, M.; Janin, A.; Lavalley, J. C.; Benazzi, E. FT infrared study of Brønsted acidity of H-mordenites: Heterogeneity and effect of dealumination. *Zeolites* **1995**, *15* (6), 507–516.
- (20) Zholobenko, V. L.; Makarova, M. A.; Dwyer, J. Inhomogeneity of Brnsted acid sites in H-mordenite. *J. Phys. Chem.* **1993**, *97* (22), 5962–5964.
- (21) Cao, K.; Fan, D.; Li, L.; Fan, B.; Wang, L.; Zhu, D.; Wang, Q.; Tian, P.; Liu, Z. Insights into the Pyridine-Modified MOR Zeolite Catalysts for DME Carbonylation. ACS Catal. 2020, 10 (5), 3372–3380.
- (22) Veefkind, V. A.; Smidt, M. L.; Lercher, J. A. On the role of strength and location of Brnsted acid sites for ethylamine synthesis on mordenite catalysts. *Appl. Catal., A* **2000**, *194–195*, 319–332.
- (23) Liu, S.; Fang, X.; Liu, Y.; Liu, H.; Ma, X.; Zhu, W.; Liu, Z. Dimethyl ether Carbonylation over Mordenite zeolite modified by Alkyimidazolium ions. *Catal. Commun.* **2020**, *147*, 106161.
- (24) Liu, S.; Liu, H.; Ma, X.; Liu, Y.; Zhu, W.; Liu, Z. Identifying and controlling the acid site distributions in mordenite zeolite for dimethyl ether carbonylation reaction by means of selective ion-exchange. *Catal. Sci. Technol.* **2020**, *10* (14), 4663–4672.
- (25) Boronat, M.; Martínez-Sánchez, C.; Law, D.; Corma, A. Enzyme-like Specificity in Zeolites: A Unique Site Position in Mordenite for Selective Carbonylation of Methanol and Dimethyl Ether with CO. *J. Am. Chem. Soc.* **2008**, *130* (48), 16316–16323.
- (26) Li, B.; Xu, J.; Han, B.; Wang, X.; Qi, G.; Zhang, Z.; Wang, C.; Deng, F. Insight into Dimethyl Ether Carbonylation Reaction over Mordenite Zeolite from in-Situ Solid-State NMR Spectroscopy. *J. Phys. Chem. C* **2013**, *117* (11), 5840–5847.
- (27) Bhan, A.; Allian, A. D.; Sunley, G. J.; Law, D. J.; Iglesia, E. Specificity of Sites within Eight-Membered Ring Zeolite Channels for Carbonylation of Methyls to Acetyls. *J. Am. Chem. Soc.* **2007**, *129* (16), 4919–4924.
- (28) Cheung, P.; Bhan, A.; Sunley, G.; Law, D.; Iglesia, E. Site requirements and elementary steps in dimethyl ether carbonylation catalyzed by acidic zeolites. *J. Catal.* **2007**, 245 (1), 110–123.
- (29) Cheung, P.; Bhan, A.; Sunley, G. J.; Iglesia, E. Selective Carbonylation of Dimethyl Ether to Methyl Acetate Catalyzed by Acidic Zeolites. *Angew. Chem., Int. Ed.* **2006**, *45* (10), 1617–1620.
- (30) Kresnawahjuesa, O.; Gorte, R. J.; White, D. Characterization of acylating intermediates formed on H-ZSM-5. *J. Mol. Catal. A: Chem.* **2004**, 208 (1–2), 175–185.
- (31) Pope, C. G. Adsorption of ethanoic acid on zeolites NaY and HY. J. Chem. Soc., Faraday Trans. 1996, 92 (19), 3647–3651.
- (32) Romotowski, T.; Komorek, J. Some aspects of interactions of methanol, acetic acid, and methylacetate with HNaZSM-5 zeolite. *Zeolites* **1991**, *11* (1), 35–41.

- (33) Gumidyala, A.; Sooknoi, T.; Crossley, S. Selective ketonization of acetic acid over HZSM-5: The importance of acyl species and the influence of water. *J. Catal.* **2016**, 340, 76–84.
- (34) Martens, J. A.; Wydoodt, M.; Espeel, P.; Jacobs, P. A. Acid-catalyzed ketonization of mixtures of low carbon number carboxylic acids on zeolite H-T. *Stud. Surf. Sci. Catal.* **1993**, *78*, 527–534.
- (35) Lezcano-González, I.; Vidal-Moya, J. A.; Boronat, M.; Blasco, T.; Corma, A. Identification of Active Surface Species for Friedel-Crafts Acylation and Koch Carbonylation Reactions by in situ Solid-State NMR Spectroscopy. *Angew. Chem., Int. Ed.* **2013**, 52 (19), 5138–5141.
- (36) Makarova, M. A.; Wilson, A. E.; van Liemt, B. J.; Mesters, C. M. A. M.; de Winter, A. W.; Williams, C. Quantification of Brønsted Acidity in Mordenites. *J. Catal.* 1997, 172 (1), 170–177.